Nephrol Dial Transplant (2000) 15: 366–374

Nephrology
Dialysis
Transplantation

Original Article

Citrate determines calcium oxalate crystallization kinetics and crystal morphology—studies in the presence of Tamm–Horsfall protein of a healthy subject and a severely recurrent calcium stone former

Bernhard Hess, Samuel Jordi, Ljerka Zipperle, Emma Ettinger[1] and Rudolf Giovanoli[1]

Department of Medicine and [1]Laboratory of Electron Microscopy, University of Berne, Berne, Switzerland

Abstract

Background. The aim of this study was to measure the effects of normal (nTHP) and abnormal stone former Tamm–Horsfall protein (SF-THP) on calcium oxalate (CaOx) nucleation and aggregation as well as on crystal morphology, in presence or absence of citrate.

Methods. Nucleation and aggregation of CaOx crystals from a supersaturated, stirred solution (200 mM NaCl, 10 mM Na-acetate, pH 5.70, 5 mM Ca and 0.5 mM Ox) were studied by spectrophotometric time-course measurements of OD at 620 nm (OD_{620}). Measured parameters were induction time t_I (time to induce formation of detectable particles), S_N, (slope of increase of OD_{620}, mainly due to crystal nucleation), and S_A, (slope of decrease of OD_{620} after equilibrium has been reached, due to crystal aggregation). Effects of citrate, nTHP and SF-THP on these parameters were measured, and scanning electron microscopy (SEM) was performed.

Results. At 1.5, 2.5 and 3.5 mM, citrate increased t_I and inhibited crystal nucleation (by 78–87%) as well as aggregation (by 63–70%), and smaller CaOx crystals (length/width ratio 1.7 ± 0.1) than under standard conditions (length/width 3.9 ± 0.5) were visible ($P < 0.001$). Normal THP at 30 and 40 mg/l inhibited crystal nucleation and, more strongly, aggregation (inhibition 76–81%). SEM revealed a decrease in length/width ratio to 2.6 ± 0.4 ($P = 0.051$ *vs* standard conditions) and less aggregation than without nTHP. At all concentrations tested, SF-THP reduced t_I ($P = 0.0001$ *vs* standard conditions) and promoted aggregation (inhibition -48 to -33%); crystals were elongated with a length/width ratio of 4.3 ± 0.6 ($P < 0.05$ *vs* nTHP). When simultaneously present with nTHP, citrate enhanced the inhibitory effects of nTHP, producing the smallest (length/width 1.5 ± 0.1) and least aggregated crystals. Finally, 3.5 mM citrate turned promotory SF-THP into a crystallization inhibitor with abundant small and clustered, but not aggregated crystals.

Conclusion. Citrate appears to be the main determinant of CaOx crystallization rates and crystal morphology in the presence of nTHP as well as SF-THP. Its effects appear to predominate over those of THP, since even promotory SF-THP is turned into a crystallization inhibitor in the presence of citrate. This re-emphasizes at a morphological level what has been concluded from functional as well from clinical studies, namely that citrate is needed in urine at equimolar concentrations to calcium in order to prevent the formation of large crystal aggregates in presence of abnormal THP.

Keywords: calcium nephrolithiasis; citrate; crystal morphology; hypocitraturia; inhibitors of crystallization; Tamm–Horsfall protein

Introduction

The initial event of stone salt precipitation is nucleation of microcrystals out of supersaturated urine [1]. Since crystal nucleation lowers urinary supersaturation without producing particles of pathophysiologically relevant sizes, it has been considered as a phenomenon of uncertain significance for stone formation [2]. Nevertheless, nucleation is an essential prerequisite for further formation of larger particles within the urinary tract which ultimately may form a stone [1].

It is by means of crystal growth and aggregation that larger particles form in renal tubules [3]. Whereas the growth of single calcium oxalate (CaOx) crystals in urine is too slow to produce particles of clinically relevant sizes [4], crystal aggregation allows for the formation of large particles at much faster rates [3,4]. Therefore, crystal aggregation appears to be the most relevant step in the formation of CaOx renal stones [3,4], and some severely recurrent stone formers are distinguished from healthy people by the fact that their urines have an abnormal propensity for forming large crystal aggregates [3]. Over the years, it has become

Correspondence and offprint requests to: PD Dr Bernhard Hess, Chief of Internal Medicine, District Hospital Zimmerberg, CH-8820 Wädenswil/Zurich, Switzerland.

clear that human urine contains many compounds which—by adsorption to surfaces of newly formed urinary crystals—alter crystal surface properties and thus the rates of crystal growth and aggregation [3]. These compounds act at concentrations much too low to affect urinary supersaturation. Most of them are macromolecules, such as glycosaminoglycans [5], Tamm–Horsfall glycoprotein (THP) [6], osteopontin [7], nephrocalcin [8], inter-α-trypsin inhibitor or bikunin [9,10], and urinary prothrombin fragment 1 [11].

Evidence has previously been presented [12–14] that normal THP (nTHP) may be a powerful inhibitor of CaOx crystal aggregation. It appears, however, that certain severely recurrent calcium renal stone formers excrete abnormal urinary THP molecules [15] which are weak inhibitors or even promoters of crystal aggregation [16]. The promotive effect of abnormal stone former THP on CaOx crystal aggregation *in vitro* goes along with the formation of larger molecular particles in comparison with nTHP, i.e. increased self-aggregation of abnormal THP molecules [15–17]. This structural–functional relationship may be reversed by citrate at concentrations equal to those in human urine [16].

We recently have developed a spectrophotometric, non-seeded supersaturation decay system which allows for separate, but not independent measurements of CaOx nucleation and aggregation in a single experiment [18]. Using this same assay system as well as scanning electron microscopy (SEM), we wanted to further assess differences between nTHP and abnormal stone former THP (SF-THP) and their interaction with citrate, especially with respect to CaOx crystallization rates and crystal morphology.

Materials and methods

Spectrophotometric crystallization measurements

Freshly prepared solutions of 10.0 mM $CaCl_2$ (Merck, Darmstadt, Germany) and 1.0 mM $K_2C_2O_4 \times H_2O$ (Merck), containing 200 mM NaCl (Merck) and 10 mM sodium acetate (Merck), were adjusted to pH 5.70 (Metrohm 654 pH-meter, Metrohm, Herisau, Switzerland). All chemicals were of the highest purity grade available. Before being used in experiments, solutions were filtered through Millex-GV membranes with a pore diameter of 0.22 μm (Millipore AG, Volketswil, Switzerland), and the calcium concentration was checked by measurements of ionized calcium, using an ion-selective electrode (Ciba-Corning Diagnostics, Medfield, MA, USA). All experiments were performed at 37°C, using a circulating water bath (Heto, Denmark). For crystallization experiments, 1.0 ml oxalate solution was transferred into a 10-mm light path quartz cuvette (Hellma No. 101, Hellma, Basle, Switzerland) placed in a Perkin-Elmer Lambda 2 spectrophotometer (Perkin-Elmer, Überlingen, Germany) connected with the circulating water bath at 37°C. In the cuvette, solutions were constantly stirred at 500 r.p.m. (Hellma Cuv-O-Stir Model 333), using a teflon-covered stirring bar, size $7 \times 2 \times 2$ mm (Semadeni, Berne, Switzerland). An additional 1.0 ml of the calcium solution was then added to obtain final concentrations of 5 mM calcium and 0.5 mM oxalate respectively.

As previously described in detail [18], automated time-course measurements of optical density at 620 nm (OD_{620}) were performed after addition of the calcium-containing solution, consisting of OD_{620} recordings every 12 s over 20 min; experiments with added inhibitors, where rates of CaOx crystal nucleation and aggregation were considerably lower, had to be extended to 40 or even 60 min. All crystallization experiments were performed at least in triplicate.

As depicted in Figure 1, the time from addition of calcium until the first detectable increment of OD_{620}, named induction time t_I, reflects the time required for CaOx crystal nuclei to form in numbers and grow into sizes which allow for detection by turbidimetry [18]. When the slope of increase of OD_{620} with time reaches its maximum, the increase in turbidity mainly reflects an increase in particle number in function of time and thus crystal nucleation; this slope is termed S_N. As already pointed out in our previous publication [18] and convincingly confirmed by a recent image analysis of CaOx crystallization studies using a very similar experimental set-up [19], increases in particle sizes, i.e. growth of crystals, always affect OD_{620} readings, especially during the second half of the steepest increase in OD_{620} with time [19].

Subsequently, an equilibrium is reached where the solution has become saturated, and crystal mass has to remain constant. However, a progressive decrease in OD_{620} with time can be observed (Figure 1) in the continuously stirred homogeneous suspension. Since total crystal mass remains constant, the decrease in OD_{620} with time must reflect a decline in particle number due to crystal aggregation, which indeed has been demonstrated by SEM [18]. Thus, the slope of decrease of OD_{620} with time in a given experiment can be taken as a measure of crystal aggregation. This slope has a negative value; for convenience − slope of decrease of OD_{620} with time, i.e. a positive number named S_A, will be used for all comparisons.

Modulators of CaOx crystallization

Citrate (Tri-potassium-citrate, Sigma Chemical Co., St Louis, MO, USA) was studied at concentrations of 1.5, 2.5 and 3.5 mM by adding the double amounts of citrate to the calcium-containing assay solution.

THP was purified according to the classical procedure with an additional passage through a molecular sieve column (Sepharose 4-B, Pharmacia, Dübendorf, Switzerland), using 4 M urea in 0.02 M sodium phosphate, pH 6.8, as eluent [16]. nTHP was isolated from a 24-h urine specimen of a 31-year-old healthy male without personal or family history of kidney stone disease whose THP had been used in a previous study of ours [16]. SF-THP was isolated from a 51-year-old man with a positive family history for stone disease who had formed 20 calcium stones. The three 24-h urine samples—that we routinely obtain from recurrent stone formers according to our previously established protocol for metabolic evaluation [20]—were pooled for further isolation and purification of THP. By adding 0.5, 1, 1.5 and 2 μg of lyophilized protein, both THPs used in this study were run on SDS-PAGE [21], using 4–15% gradient gels (Mini Protean II, Bio-Rad, Glattbrugg, Switzerland) on a Mini Trans-Blot apparatus (Bio-Rad), and stained with silver stain (Bio-Rad).

For crystallization experiments, aqueous suspensions (2 ml) with excess lyophilized THP were prepared and then centrifuged for 10 min at 4000 r.p.m. in a Heraeus Christ

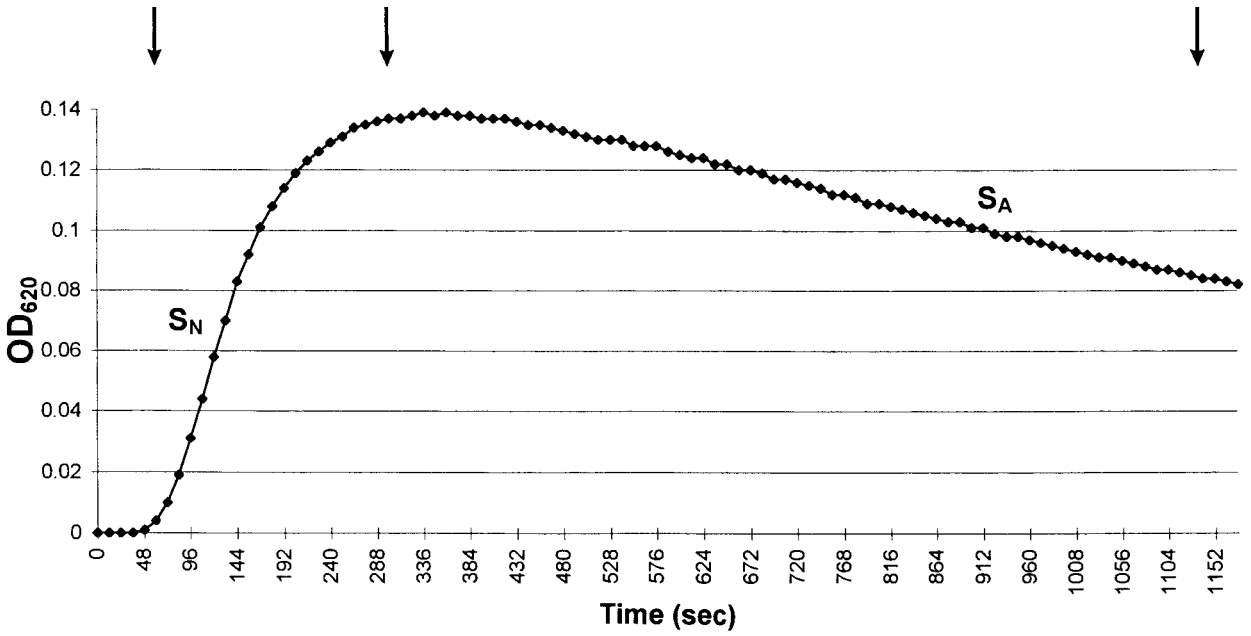

Fig. 1. Time-course measurements of OD_{620} in a control experiment at standard conditions (calcium 5.0 mM, oxalate 0.5 mM). S_N, maximum slope of increase of OD_{620} with time, i.e. maximum rate of crystal nucleation. S_A, maximum slope of decrease of OD_{620} with time, i.e. maximum rate of crystal aggregation. Arrows mark time-points where 30-µl-aliquots were taken for SEM studies (see *Materials and Methods*).

Biofuge A (Heraeus, Zurich, Switzerland). Thereafter, THP concentration in the supernatant was measured spectrophotometrically at 277 nm [15,16]. After 1.0 ml of oxalate-containing solution had been added to the cuvette, small volumes (<5 vol%) of these concentrated THP solutions were injected into the oxalate-containing solution, before the calcium-containing solution was added and the experiment was started. THP was tested at concentrations of 20, 30 and 40 mg/l.

Percentage inhibition in the presence of citrate or either form of THP was calculated as

$[1-(S_{Nm}/S_{Nc})] \times 100$ for the rate of nucleation,

$[1-(S_{Am}/S_{Ac})] \times 100$ for the rate of aggregation,

respectively, where m stands for modulator and c for control [18]. Negative inhibition values indicate promotion of the respective crystallization process.

SEM

During induction time as well as at the end of maximum increase of OD_{620} (ΔOD_{max}, i.e. combined nucleation and growth) and at the end of maximum decrease of OD_{620} with time ($-\Delta OD_{max}$, i.e. aggregation), 30 µl of assay solution were transferred from the spectrophotometric cuvette onto a Millipore GV filter membrane, diameter 47 mm, of pore size 0.22 µm (Millipore AG) under vacuum, as previously described [18]. Samples for SEM were taken from experiments under standard conditions (no modulator added), with 3.5 mM citrate, with 30 mg/l of either nTHP or SF-THP, and with 30 mg/l of nTHP together with 3.5 mM citrate or 30 mg/l of SF-THP together with 3.5 mM citrate. For drying, filters were cut to size and mounted on an aluminum holder by means of a double-sided graphitized adhesive tab. A gold layer about 400 Å thick was then sputtered onto the sample. Specimens were investigated using a JEOL JSM-840 scanning electron microscope with an acceleration voltage of 25 kV and a working distance between 15 and 25 mm. Photographs were taken at magnifications of ×250, ×1000 and ×5000 respectively.

On representative fields of photographs (10 × 13 cm) taken at 250-fold magnification during induction time as well as during ΔOD_{max} and during $-\Delta OD_{max}$, total numbers of particles were counted three times on three different days by one of us (B.H.), whereby single crystals were distinguished from aggregates (defined as many crystals sticking together and forming one particle) and clusters (accumulations of many loose single crystals). In addition, maximum lengths and widths of all distinct particles on photographs (10 × 13 cm) taken at 1000-fold magnification towards the end of $-\Delta OD_{max}$ were measured, and length/width ratios were calculated.

Statistics

All values are means ± SE. Unpaired and paired *t*-test for comparisons between and within groups respectively, were used.

Results

Normal and SF-THP on SDS–PAGE

As depicted in Figure 2, both glycoproteins migrated as a single band at about 80 kDa on SDS–PAGE (note that proteins are overexposed at highest concentrations).

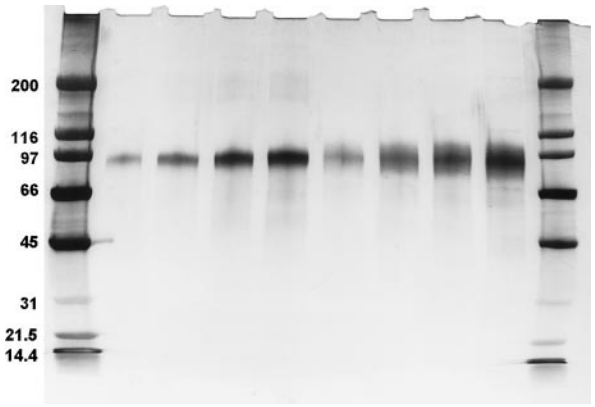

Fig. 2. PAGE of nTHP and SF-THP. From left to right: lane 1, molecular weight markers (numbers are kDa); lanes 2–5, THP at 0.5, 1.0, 1.5 and 2.0 μg; lanes 6–9, SF-THP at 0.5, 1.0, 1.5 and 2.0 μg; lane 10, molecular weight markers.

Crystallization studies

In CaOx crystallization experiments under standard conditions without modulators (15 experiments), induction time was 61.9 ± 1.9 s, rate of nucleation (S_N) $1.058 \pm 0.042 \times 10^{-3}$/s, and rate of aggregation (S_A) $0.067 \pm 0.008 \times 10^{-3}$/s.

Table 1 summarizes induction times (t_I) in presence of various crystallization modulators. Citrate at all three concentrations studied significantly prolonged t_I to values between 98 and 126 s. Whereas nTHP did not affect t_I, SF-THP significantly reduced it at all concentrations studied ($P = 0.0001$ for all comparisons *vs* standard conditions), indicating promotion of nucleation in comparison with standard conditions. Finally, when 3.5 mM citrate was present together with either form of THP, induction time was significantly longer than with citrate alone; this indicates strong potentiation of nTHP effects and even reversal of promotory effects of SF-THP by citrate.

Citrate at 1.5 (number of experiments = 7), 2.5 ($n = 8$) and 3.5 mM ($n = 8$) inhibited nucleation of CaOx crystals by 82.1 ± 1.0, 78.0 ± 1.0 and 86.5 ± 0.9% respectively, and aggregation by 62.7 ± 1.5, 62.7 ± 1.5 and 70.2 ± 1.5% respectively ($P = 0.0001$ for all comparisons between any citrate concentration and standard conditions, both for nucleation and aggregation). Figure 3 depicts findings with both forms of THP: nTHP moderately inhibited crystal nucleation only at 30 and 40 mg/l, whereas aggregation was greatly inhibited at all concentrations that we tested ($P < 0.005$ for all concentrations *vs* standard conditions without nTHP). On the other hand, SF-THP did not significantly affect the rate of nucleation, whereas crystal aggregation was clearly promoted (negative inhibition values between -33 and -48%) at all concentrations of SF-THP that we studied ($P < 0.01$ for all comparisons *vs* standard conditions without SF-THP).

Experiments with nTHP or SF-THP combined with citrate were carried out with 30 mg/l of either THP and 3.5 mM citrate, as summarized in Figure 4. The addition of citrate significantly increased inhibition of

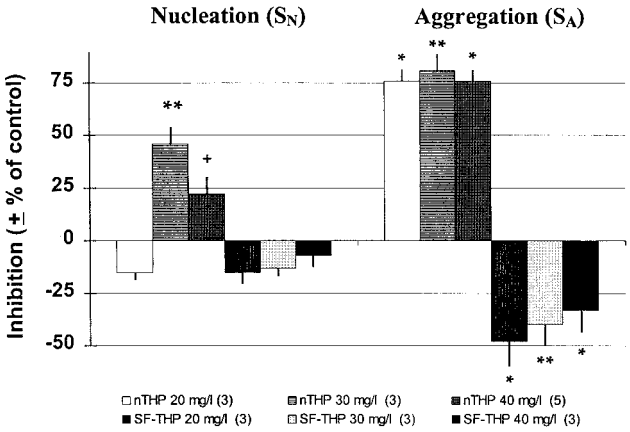

Fig. 3. Inhibition of nucleation (S_N) and aggregation (S_A) of CaOx crystals by either THP or abnormal SF-THP at three concentrations. Numbers in parentheses are numbers of experiments. $^+$, $P < 0.025$; *, $P < 0.01$; **, $P < 0.001$ *vs* standard conditions.

Table 1. Induction times (t_i) under various experimental conditions

Experimental condition	Induction time (t_i) (s)	Significances
Standard (15)	61.9 ± 1.9	
CIT 1.5 mM (7)	97.7 ± 11.9	**
CIT 2.5 mM (8)	125.9 ± 4.3	**
CIT 3.5 mM (8)	109.9 ± 3.0	**
nTHP 20 mg/l (3)	58.7 ± 8.4	NS *vs* standard
nTHP 30 mg/l (3)	63.3 ± 11.1	NS *vs* standard
nTHP 40 mg/l (3)	56.8 ± 6.4	NS *vs* standard
SF-THP 20 mg/l (3)	37.0 ± 1.7	**, NS *vs* nTHP
SF-THP 30 mg/l (3)	30.7 ± 2.7	**, $^\circ$
SF-THP 40 mg/l (3)	31.0 ± 4.6	**, $^\circ$
nTHP 30 mg/l + 3.5 mM CIT (3)	179.3 ± 11.3	$^+$
SF-THP 30 mg/l + 3.5 mM CIT (4)	183.3 ± 16.3	$^{++}$

t_i is the time required for CaOx crystal nuclei to reach numbers and sizes which allow for detection by turbidimetry. Numbers in parentheses, numbers of experiments.
**, $P < 0.001$ *vs* standard conditions; $^\circ$, $P < 0.05$ *vs* nTHP; $^+$, $P < 0.01$ and $^{++}$, $P < 0.001$ *vs* same THP without citrate.

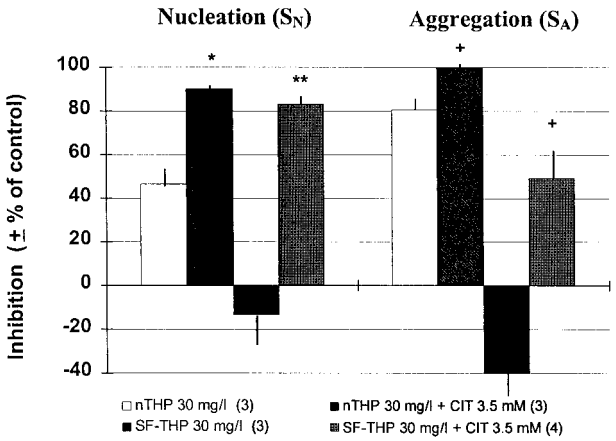

Fig. 4. Effect of 3.5 mM citrate on inhibition of S_N and S_A of CaOx crystals by either nTHP or abnormal SF-THP at 30 mg/l. Numbers in parentheses are numbers of experiments. $^+$, $P<0.025$; *, $P<0.005$; **, $P<0.001$ *vs* without citrate.

nucleation and aggregation by normal THP and turned promotive SF-THP into an inhibitor.

SEM

Figure 5 depicts representative fields of photographs at 1000-fold magnification taken at the end of experiments, i.e. during maximum rates of aggregation. As depicted in Table 2, maximum length and width of particles under standard conditions (Figure 5A) amounted to 11.5 ± 1.7 and 3.1 ± 0.3 μm respectively, and the length/width ratio was 3.9 ± 0.5. In the presence of 3.5 mM citrate (Figure 5B), the length/width ratio was highly significantly reduced due to a significant reduction in particle length. With 30 mg/l of nTHP (Figure 5C), there was heterogeneity of particle sizes, but a fall in the mean length/width ratio at the limit of significance ($P=0.051$) was noted in comparison with standard conditions, due to a decrease in mean particle length. On the other hand, 30 mg/l of SF-THP (Figure 5D) tended to produce significantly longer and more aggregated crystals than nTHP; in comparison with standard conditions, however, particle sizes were not significantly affected by SF-THP. In the presence of both 3.5 mM citrate and 30 mg/l nTHP (Figure 5E), crystals were of similar shape than with citrate alone, reflected also by a similar length/width ratio; the latter was significantly lower than with nTHP alone. Finally, 3.5 mM citrate and 30 mg/l SF-THP (Figure 5F) produced abundant crystals as small as with citrate alone; these crystals were often clustered, but not aggregated.

At 5000-fold magnification, Figure 6 clearly demonstrates the impact of citrate on the effects of abnormal SF-THP: whereas proteinaceous material at the crystal surfaces appears to aggregate crystals like a glue (Figure 6A), the same experiment performed with an additional 3.5 mM of citrate produces much smaller and non-aggregated crystals (Figure 6B). Again, the shape of crystals in presence of citrate is clearly different from crystals obtained under control conditions or in presence of THP.

Table 3 summarizes particle countings on representative photographs taken at 250-fold magnification under six different experimental conditions. The decrease of total particle number due to aggregation under standard conditions (no modulator added) was totally abolished by citrate where particle number remained stable throughout the whole experiment. Whereas citrate tended to reduce particle number during $\Delta OD_{620\ max}$ ($P=0.056$ *vs* standard conditions), a rise in particle number was observed during $-\Delta OD_{620\ max}$ ($P=0.028$ *vs* standard conditions), indicating inhibition of crystal nucleation as well as aggregation. The same was true for nTHP: particle numbers during $\Delta OD_{620\ max}$ fell in comparison with standard conditions ($P=0.003$), whereas they rose during $-\Delta OD_{620\ max}$ ($P=0.016$ *vs* standard conditions). On the other hand, SF-THP increased particle number during $\Delta OD_{620\ max}$ ($P=0.003$ *vs* standard conditions), indicating promotion of nucleation, whereas the numerous crystal aggregates found during $-\Delta OD_{620\ max}$ made countings of distinct particles impossible (see also Figures 5D and 6A). Fewer particles were nucleated during $\Delta OD_{620\ max}$, when nTHP and citrate were simultaneously present ($P=0.009$ *vs* standard conditions). On the other hand, the combination of SF-THP and citrate increased the number of nucleated particles ($P=0.009$ *vs* standard conditions), whereas counting at 250-fold magnification became impossible in samples taken during $-\Delta OD_{620\ max}$, due to cluster formation.

Discussion

Although results obtained with THPs from one healthy control and one severely recurrent CaOx renal stone former do not allow for generalized conclusions, several important findings emerge from this *in vitro* study: (i) under the experimental conditions of the present experiments, citrate is the main determinant of CaOx crystallization kinetics and crystal morphology; (ii) nTHP is not only an inhibitor of CaOx crystal aggregation (as previously demonstrated [12,16]), but—to a somewhat lesser degree—also of nucleation, whereas abnormal SF-THP promotes both nucleation and aggregation of CaOx crystals; and (iii) citrate reverses promotory effects of abnormal THP into inhibition of CaOx crystal nucleation and aggregation.

By chelation of calcium ions, citrate efficiently lowers supersaturation, the driving force for crystallization [1,22]. Citrate in a supersaturation decay system is therefore expected to reduce induction time and rate of nucleation. In addition, citrate at the urine-like concentrations tested herein also inhibits crystal aggregation. This is in apparent contradiction to our previous findings under saturated conditions [12] where citrate did not affect the rate of crystal aggregation. However, whereas experiments in the present study start from a high CaOx supersaturation, our previous work was performed at permanently saturated solution conditions [12,15,16], with a calcium concentration of

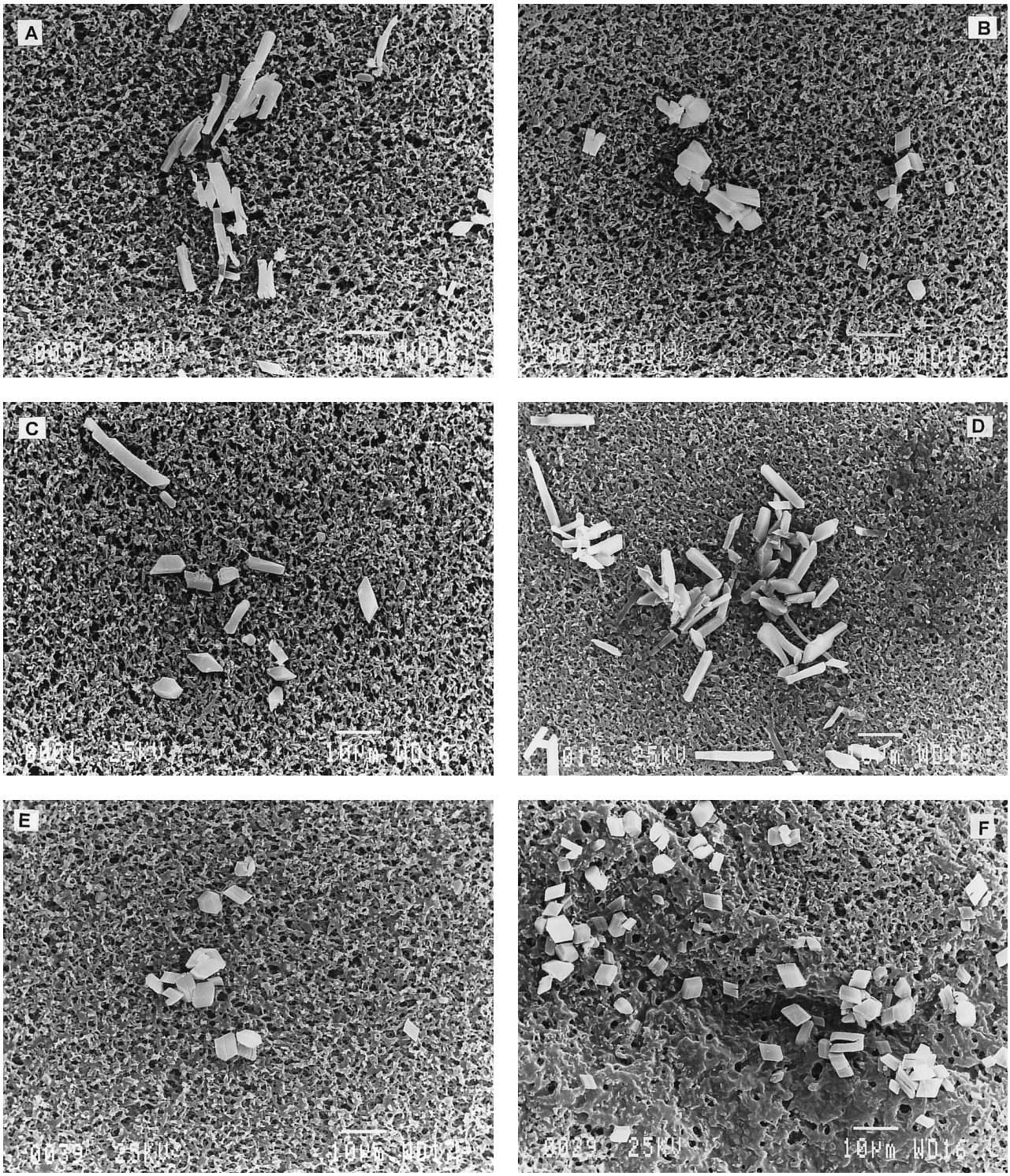

Fig. 5. Photographs taken from SEM preparations at $\times 1000$ magnification under six various experimental conditions during crystal aggregation (maximum decrease of OD_{620} with time, figure 1). (**A**) standard conditions (Calcium 5.0 mM, Oxalate 0.5 mM); (**B**) +3.5 mM citrate; (**C**) +30 mg/l nTHP; (**D**) +30 mg/l SF-THP; (**E**) +30 mg nTHP+3.5 mM citrate; and (**F**) +30 mg/l SF-THP+3.5 mM citrate. For details, see text. Bars = 10 μm.

only 0.14 mmol/l. This was most probably too low for abundant formation of calcium–citrate complexes which bind to specific sites on CaOx crystal surfaces and are thus crucial for lowering rates of crystal growth and aggregation [22]. Therefore, formation of significant numbers of calcium–citrate complexes may best explain crystal aggregation inhibition by citrate in the present study.

Table 2. Maximum lengths and widths, respectively, and length/width ratios of crystalline particles on photographs taken at 1000-fold SEM magnifications. The samples were taken at the end of crystallization experiments (maximum aggregation) under six various experimental conditions

Experimental condition	Max. length (μm)	Max. width (μm)	Length/width
Standard	11.5 ± 2.7	3.1 ± 0.3	3.9 ± 0.5
CIT 3.5 mM	5.2 ± 0.4***	3.2 ± 0.2	1.7 ± 0.1***,$^{++}$
nTHP 30 mg/l	7.1 ± 1.1*	2.8 ± 0.2	2.6 ± 0.4$^{\times}$
SF-THP 30 mg/l	12.0 ± 1.2$^{+++,000}$	4.1 ± 1.0	4.3 ± 0.6$^{+,000}$
nTHP 30 mg/l + CIT 3.5 mM	5.4 ± 0.3**	3.9 ± 0.3	1.5 ± 0.1^{++},**
SF-THP 30 mg/l + CIT 3.5 mM	5.2 ± 0.2***	3.3 ± 0.2	1.7 ± 0.1***

$^{\times}P = 0.051$; $^{*}P < 0.05$; $^{**}P < 0.01$; $^{***}P < 0.001$ *vs* standard conditions; $^{+}P < 0.05$; $^{++}P < 0.025$; $^{+++}P < 0.01$ *vs* nTHP; $^{000}P < 0.001$ *vs* SF-THP 30 mg/l + citrate 3.5 mM.

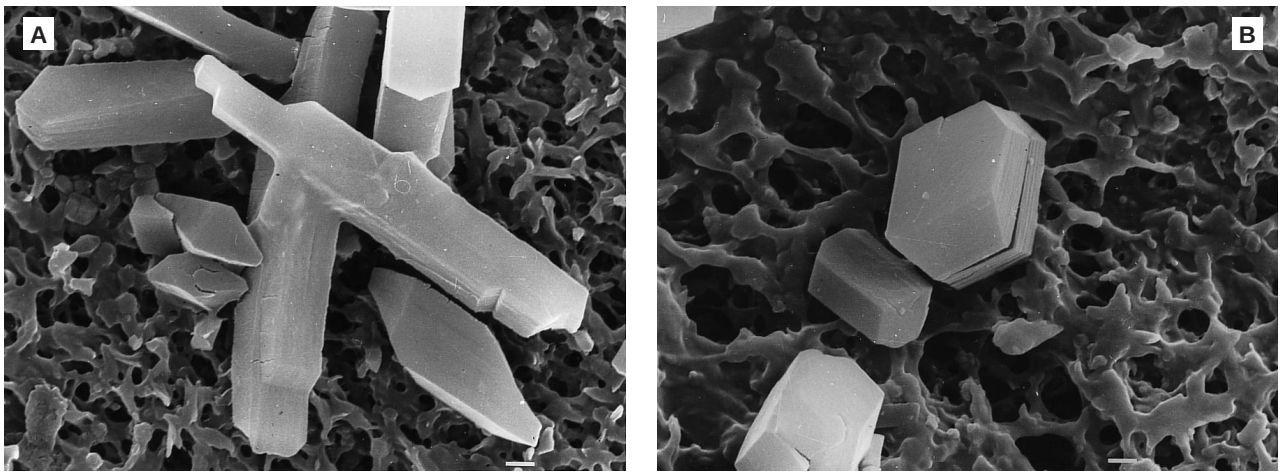

Fig. 6. Photographs taken from SEM preparations at ×5000 magnification in presence of 30 mg/l SF-THP (**A**) and 30 mg/l SF-THP + 3.5 mM citrate (**B**). For details, see text. Bars = 1 μm.

Table 3. Countings of crystalline particles on photographs taken at 250-fold SEM magnifications of samples taken at various times during crystallization experiments

Experimental condition	Particles/field, counted during		
	Induction time	$\Delta OD_{620\ max.}$	$-\Delta OD_{620\ max.}$
Standard	0	70.7 ± 2.7	41.7 ± 0.3^{++}
CIT 3.5 mM	4	57.0 ± 4.4	59.3 ± 5.2*
nTHP 30 mg/l	5	49.7 ± 1.7****	61.3 ± 4.9**
SF-THP 30 mg/l	14	109.0 ± 5.0****	aggregates
nTHP 30 mg/l + CIT 3.5 mM	0	53.3 ± 1.3***	46.7 ± 3.9
SF-THP 30 mg/l + CIT 3.5 mM	3	134.3 ± 13.2***	clusters

Numbers are crystalline particles per photographic field on photographs of 9 × 12 cm. All countings of particles, which were impossible in presence of SF-THP and SF-THP+ citrate, were done in *triplicate*. Induction time, time before crystals reach sizes/numbers which make them detectable by turbidimetry; $\Delta OD_{620\ max.}$, end of max. increase of OD_{620} with time, i.e. mainly combined nucleation and growth; $-\Delta OD_{620\ max.}$, end of max. decrease of OD_{620} with time, i.e. mainly aggregation. For details, see text.
$^{*}P < 0.05$; $^{**}P < 0.025$; $^{***}P < 0.01$; and $^{****}P < 0.005$ *vs* standard conditions. $^{++}P < 0.01$ vs $\Delta OD_{620\ max}$.

Inhibition by citrate at the urine-like concentrations that we used in this in-vitro study is not concentration-dependent. This is in keeping with results previously obtained by Kok *et al.* [23] who, using a crystallization system very different from ours, also could not find dose-dependent inhibition of crystal growth and aggregation at millimolar concentrations of citrate. In their study, inhibition only became dose-dependent at citrate concentrations below 1.0 mM [23]. Obviously citrate reaches its maximum effect on CaOx crystallization *in vitro* at millimolar, i.e. urine-like, concentrations. Very similar to the recent findings of Hennequin *et al.* [19], our SEM studies provide evidence that citrate at millimolar concentrations has two main

effects on newly forming CaOx particles *in vitro*, namely (i) precipitation of significantly smaller crystals and (ii) reduced aggregate formation.

In accordance with our previous findings [12,15,16], nTHP is a strong inhibitor of the aggregation of CaOx crystals also under the highly supersaturated conditions of the present experiments. Whereas rather elongated CaOx crystals, similar to those described by Hennequin *et al*. [19,24], formed under standard conditions, nTHP inhibited both nucleation and aggregation, i.e. produced fewer, smaller and less aggregated crystals. This is in accordance with a most recent study by Hallson *et al*. [25] who demonstrated inhibition of CaOx and calcium phosphate crystal aggregation by normal human THP in ultrafiltered human urines evaporated to 800 mosmol/kg. On the other hand, THP obtained from a severely recurrent calcium stone former promoted both nucleation and aggregation of CaOx crystals. To our knowledge, the present study is the first to investigate crystallization kinetics as well as the morphology of CaOx crystals precipitated in presence of abnormal SF-THP.

It is well known that at high ionic strength, low pH and high calcium concentrations such as in the present study, abnormal SF-THP may flocculate and form highly gel-like particles [16,17]. These flocks not only act as nucleators, but also induce aggregation by trapping CaOx crystals like a glue [14], as demonstrated by our SEM studies (Figure 6A). The structural basis of this functional abnormality remains to be elucidated. As recently demonstrated by Hallson *et al*. [25], the functional properties of THP molecules might be affected by their sialic acid content.

Our study demonstrates that citrate potentiates the effects of THP: when citrate is present in addition to normal THP, THP inhibition of crystallization is enhanced, and length/width ratios of precipitated crystals are significantly lowered in comparison with nTHP alone (Table 2). These findings confirm our previous *in vitro* studies, where citrate enhanced inhibitory effects of nTHP [16], also at a morphological level. Even more exciting from a clinical point of view is the fact that citrate turns abnormal SF-THP from a promoter of crystallization into a strong inhibitor. Previously, we have demonstrated that citrate diminishes exaggerated self-aggregation of abnormal THP molecules by lowering free calcium concentration, as evidenced by viscosity measurements and equilibrium centrifugation [15,16]. Moreover, altered functional properties of abnormal SF-THP molecules as modulators of CaOx crystallization were directly related to the observed conformational changes [16]. The present study again confirms these findings at a morphological level, since citrate in presence of SF-THP allows for the formation of much smaller and less aggregated CaOx crystals than SF-THP alone.

In conclusion, under the supersaturated conditions of this in-vitro study, citrate at physiologic concentrations is a main determinant of rates of CaOx nucleation and aggregation as well as of crystal morphology. Its effects appear to predominate over those of THP: the presence of citrate improves inhibitory activity of nTHP and turns promotory SF-THP into an inhibitor of crystallization, leading to formation of smaller and less aggregated crystals. This re-emphasizes at a morphological level what has been concluded from functional studies [16] as well as from a clinical point of view [26], namely that citrate is needed in urine at equimolar concentrations to calcium in order to prevent the formation of large crystal aggregates in presence of abnormal THP.

Acknowledgements. The authors thank Beatrice Frey, Laboratory of Electron Microscopy, for technical assistance. This study has been supported by the Swiss National Science Foundation (Grant No. 32-43448.95) to B.H.

References

1. Finlayson B. Physicochemical aspects of urolithiasis. *Kidney Int* 1978; 13: 344–360
2. Coe FL, Parks JH, Nakagawa Y. Protein inhibitors of crystallization. *Semin Nephrol* 1991; 11: 98–109
3. Hess B, Kok DJ. Nucleation, growth and aggregation of stone-forming crystals. In: Coe FL, Favus MJ, Pak CYC, Parks JH, Preminger GM, eds. *Kidney Stones: Medical and Surgical Management*. Lippincott-Raven Publishers, Philadelphia: 1996: 3–32
4. Kok DJ, Khan SR. Calcium oxalate nephrolithiasis, a free or fixed particle disease. *Kidney Int* 1994; 46: 847–854
5. Hesse A, Wuzel H, Vahlensieck W. Significance of glycosaminoglycans for the formation of calcium oxalate stones. *Am J Kidney Dis* 1991; 27: 414–419
6. Hess B. Tamm–Horsfall glycoprotein and calcium nephrolithiasis. *Miner Electrolyte Metab* 1994; 20: 393–398
7. Hoyer JR. Uropontin in urinary calcium stone formation. *Miner Electrolyte Metab* 1994; 20: 385–392
8. Coe FL, Nakagawa Y, Asplin J, Parks JH. Role of nephrocalcin in inhibition of calcium oxalate crystallization and nephrolithiasis. *Miner Electrolyte Metab* 1994; 20: 378–384
9. Dawson CJ, Grover PK, Ryall RL. Inter-α-inhibitor in urine and calcium oxalate urinary crystals. *Brit J Urol* 1998; 81: 20–26
10. Atmani F, Mizon J, Khan S. Identification of uronic-acid-rich protein as urinary bikunin, the light chain of inter-α-inhibitor. *Eur J Biochem* 1996; 236: 984–990
11. Stapleton AME, Ryall RL. Crystal matrix protein—getting blood out of a stone. *Miner Electrolyte Metab* 1994; 20: 399–409
12. Hess B, Nakagawa Y, Coe FL. Inhibition of calcium oxalate monohydrate crystal aggregation by urine proteins. *Am J Physiol* 1989; 257: F99–106
13. Ryall R, Harnett RM, Hibberd CM, Edyvane KA, Marshall VR. Effects of chondroitin sulphate, human serum albumin and Tamm–Horsfall mucoprotein on calcium oxalate crystallization in undiluted human urine. *Urol Res* 1991; 19: 181–188
14. Scurr DS, Robertson WG. Modifiers of calcium oxalate crystallization found in urine. II. Studies on their mode of action in an artificial urine. *J Urol* 1986; 136: 128–131
15. Hess B, Nakagawa Y, Parks JH, Coe FL. Molecular abnormality of Tamm–Horsfall glycoprotein in calcium oxalate nephrolithiasis. *Am J Physiol* 1991; 260: F569–578
16. Hess B, Zipperle L, Jaeger Ph. Citrate and calcium effects on Tamm–Horsfall glycoprotein as a modifier of calcium oxalate crystal aggregation. *Am J Physiol* 1993; 265: F784–791
17. Boevé ER, Cao LC, de Bruijn WC, Robertson WG, Romijn JC, Schroeder FH. Zeta potential distribution on calcium oxalate crystal and Tamm–Horsfall protein surface analyzed with Doppler electrophoretic light scattering. *J Urol* 1994; 152: 531–536
18. Hess B, Meinhardt U, Zipperle L, Giovanoli R, Jaeger Ph. Simultaneous measurements of calcium oxalate crystal nucleation and aggregation: impact of various modifiers. *Urol Res* 1995; 23: 231–238

19. Hennequin C, Lalanne V, Drüeke T, Daudon M, Lacour B. Validation by image analysis of a turbidimetric method to study calcium oxalate crystallization. *Clin Nephrol* 1997; 48: 292–299
20. Hess B, Hasler-Strub U, Ackermann D, Jaeger Ph. Metabolic evaluation of patients with recurrent idiopathic calcium nephrolithiasis. *Nephrol Dial Transplant* 1997; 12: 1362–1368
21. Laemmli UK. Cleavage of structural proteins during the assembly of the head of bacteriophage T4. *Nature* 1970; 227: 680–685
22. Tiselius H-G. Solution chemistry of supersaturation. In: Coe FL, Favus MJ, Pak CYC, Parks JH, Preminger GM, eds. *Kidney Stones: Medical and Surgical Management*. Lippincott-Raven Publishers, Philadelphia: 1996: 33–64
23. Kok DJ, Papapoulos SE, Blomen LJMJ, Bijvoet OLM. Modulation of calcium oxalate monohydrate crystallization kinetics in vitro. *Kidney Int* 1988; 34: 346–350
24. Hennequin C, Lalanne V, Daudon M, Lacour B, Drueke T. A new approach to studying inhibitors of calcium oxalate crystal growth. *Urol Res* 1993; 21: 101–108
25. Hallson PC, Choong SKS, Kasidas GP, Samuell CT. Effects of Tamm–Horsfall protein with normal and reduced sialic acid content upon crystallization of calcium phosphate and calcium oxalate in human urine. *Br J Urol* 1997; 80: 533–538
26. Erwin DT, Kok DJ, Alam J *et al*. Calcium oxalate stone agglomeration reflects stone-forming activity: citrate inhibition depends on macromolecules larger than 30 kilodalton. *Am J Kidney Dis* 1994; 24: 893–900

Received for publication: 4.12.98
Accepted in revised form: 24.7.99